



Research Article

The effects of silver nanoparticles biosynthesized using fig and olive extracts on cutaneous *leishmaniasis*-induced inflammation in female balb/c mice

 Mina A. Almayouf¹,  Manal El-khadragy^{2,3}, Manal A. Awad⁴ and Ebtesam M. Alolayan¹

¹Faculty of Science, Zoology Department, King Saud University, Riyadh 11451, Saudi Arabia; ²Biology Department, Faculty of Science, Princess Nourah Bint Abdulrahman University, Riyadh 11671, Saudi Arabia; ³Department of Zoology and Entomology, Faculty of Science, Helwan University, Cairo 11795, Egypt; ⁴King Abdullah Institute for Nanotechnology, King Saud University, Riyadh 11451, Saudi Arabia

Correspondence: Mina A. Almayouf (Almayouf.m@hotmail.com)



Leishmaniasis is a group of infectious and noncontagious severe parasitic diseases, caused by protozoans of the *Leishmania* genus. Natural products characterize a rich source of prospective chemical entities for the development of new effective drugs for neglected diseases. Scientific evaluation of medicinal plants has made it possible to use some metabolites from flavonoids and polyphenols compounds for the treatment of parasitic diseases. Therefore, we aimed in the present study to evaluate the protective effect of silver nanoparticles (Ag-NPs) biosynthesized using Fig and Olive extracts (NFO) against Cutaneous *leishmaniasis* in female Balb/c mice. A total of 70 mice were used and divided into seven groups. Treatment was initiated when local lesions were apparent, we found that Fig and Olive extracts were found to be a good source for the synthesis of (Ag-NPs), their formation was confirmed by color change and stability in solution. Nanoparticles biosynthesized using Fig and Olive extracts induced a reduction in the average size of cutaneous leishmaniasis lesions compared with the untreated mice. Moreover, nanoparticles treatment decreased oxidative stress (LPO, NO), down-regulation gene expression levels (*TNF- α* , *IL-1 β* , and *BAX*), and this antileishmanial activity of nanoparticles was associated with enhanced antioxidant enzyme activities. In addition, histopathological evaluation proved the antileishmanial activity of nanoparticles compared with the positive control.

Therefore, we aimed in the present study to evaluate the protective effect of silver nanoparticles biosynthesized using Fig and Olive extracts against cutaneous lesions induced by *Leishmania major* infection through their anti-inflammatory, antioxidant activities, and faster clinical efficacy than standard pentavalent antimonial treatment.

Introduction

Leishmaniasis is a parasitic disease caused by infection with protozoan parasites of the genus *Leishmania*, which spread by biting of infected female sand flies [1]. The genus *Phlebotomus* is considered the vector of *leishmaniasis* [2]. Several forms of *leishmaniasis* have been detected including Cutaneous *leishmaniasis* (CL), Mucocutaneous *leishmaniasis* (MCL), and Visceral *leishmaniasis* (VL) [3].

CL spreads all over the Kingdom of Saudi Arabia with greatly varying prevalence rates in different regions. According to the Ministry of Health statistical yearbook, in 2018, Al-Qassim region presented the highest percentage of the total number of cases (17.4%), followed by Al-Medinah (16.6%), and then Al-Ahsa (13.4%). CL lesions usually resolve spontaneously in a few months (without treatment). However,

Received: 29 July 2020
Revised: 20 November 2020
Accepted: 24 November 2020

Accepted Manuscript online:
30 November 2020
Version of Record published:
16 December 2020

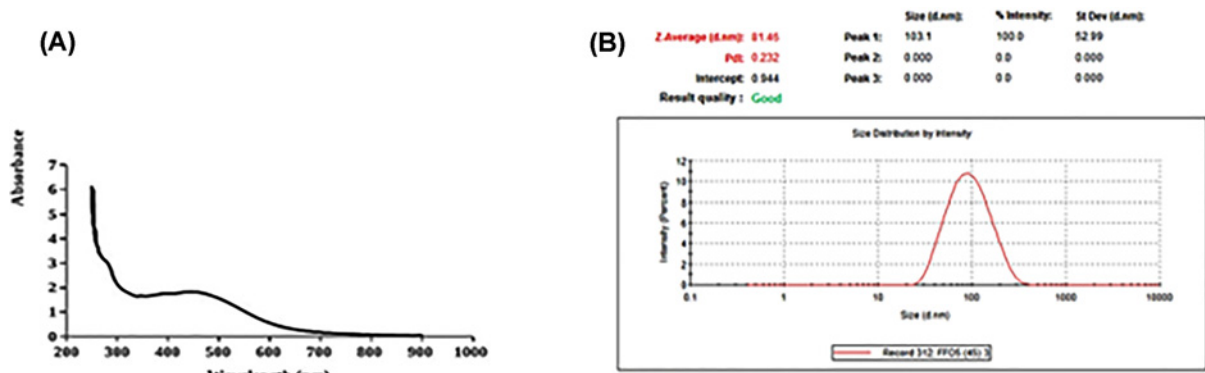


Figure 1. Determination of the synthesis of silver nanoparticles

(A) The absorption spectrum of the (NFO). (B) Figure present a graph produced by using a zeta sizer for measuring the average size of (NFO).

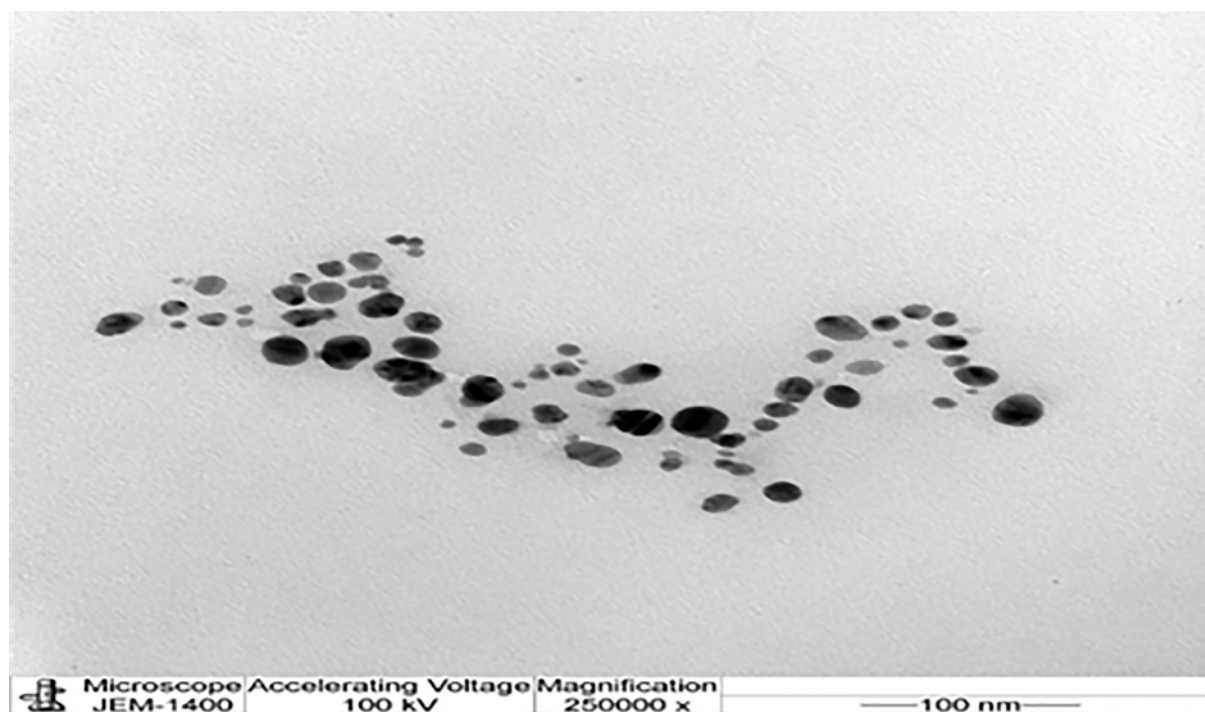


Figure 2. Determination of silver nanoparticles by transition electron microscopy (TEM)

Figure presents a transition electron microscopy (TEM) image of (NFO) (scale bar: 100 nm).

a disfiguring scar may remain at the infection site due to slow healing and may lead to self-stigma and social stigma and have negative psychological effects on the young [4]. The currently used pentavalent antimony drugs, such as pentamidine and amphotericin B, may display toxicity, and have also unpleasant side effects. Furthermore, parasite may develop resistance to treatment. Therefore, the lack of vaccines, the emergence of drug resistance and the adverse effects of currently used drugs emphasize the need to discover novel drugs, particularly from natural products. Efforts to find alternative cost effective, nontoxic drugs against *leishmaniasis* have led to the development of a few potential drugs from natural resources [5].

The use of natural products as combinations (blends) is a common practice in Saudi Arabia and has existed in many cultural systems for centuries [6]. Natural products provide prototypes for pharmacologically active compounds, particularly as antimicrobial, anticancer, and antiparasitic agents. Several internal or external pathological factors

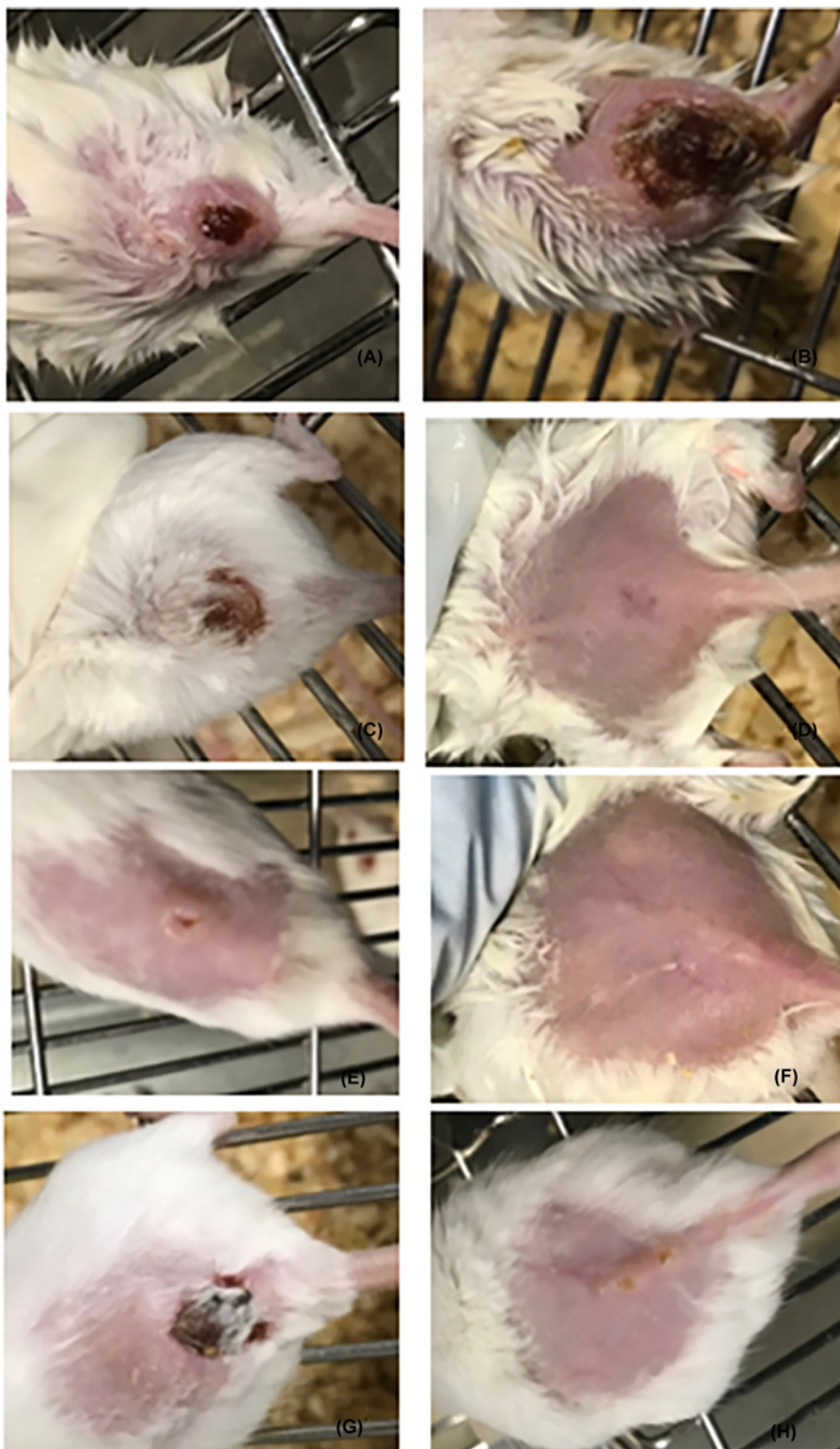


Figure 3. Lesion size of infected and treated mice

CL lesions of infected mice (A) first week in (PC) mice showing redness, swelling, and ulcer formation. (B) Fourth week of (PC) mice showing redness, swelling, ulcer, and gangrene formation. (C) First week post-treatment with Pentostam showing redness, swelling, ulcer, and gangrene formation. (D) Fourth week post treatment with Pentostam showing complete recovery with scar formation. (E) First week post treatment with NFOA. (F) Third week post treatment with NFOA showing restored to normal skin. (G) First week post treatment with FOA. (H) 4th week post treatment with FOA showing restored to normal skin with small ulcer.

such as parasitic infections interrupt the oxidant/antioxidant balance, leading to oxidative stress. The antioxidant defense system is closely connected with nutrition [7,8].

Synthesis of silver nanoparticles (Ag-NPs) utilizing fungi, bacteria, or plant extracts has emerged as an alternative approach. There are several reasons for interest in green biosynthetic methods for (Ag-NPs). They are simple, cost-effective, provide large quantities, are harmless and environmentally friendly [9]. The reduction and stabilization of silver ions is achieved by combining biomolecules such as amino acids, proteins, enzymes, alkaloids, polysaccharides, phenolics, tannins, vitamins and saponins, from plant extracts that are already established as having therapeutic value [10]. In recent years, they have attracted considerable attention for chemical and medical applications due to their exceptional properties including anti-inflammatory, antibacterial, and antiparasitic activities, high resistance to oxidation and promotion of wound healing [11,12]. Biosynthesis of (Ag-NPs) has been carried out by utilizing ethanol extracts from *Cardiospermum halicacabum* L. leaves [13], *Impatiens balsamina* L. leaves [14], and *Lantana camara* L. fruits [15]. Psoralen is a novel compound that is used to reduce pathological effects of *L. major*, *L. infantum*, and *L. chagasi* promastigotes. Also, Oleuropein derived from the Olive tree, *Olea europaea* L. (Oleaceae), is a biophenol with many biological activities. A previous study has shown that Oleuropein exhibits leishmanicidal effects against three *Leishmania* spp. *in vitro* and minimizes the parasite burden in *L. donovani*-infected Balb/c mice [16].

Ficus carica Linn is an Asian and Middle East species of flowering plant that belong to the mulberry family. It contains high levels of anthocyanins, polyphenols (such as Psoralen), and flavonoids, are exhibits good antioxidant capacity and pharmacological actions including antioxidant, antibacterial, anti-inflammatory, gastroprotective, vulnerary, anticancer, antispasmodic, antiparasitic, and immunobalancing activities [17–20]. The Psoralen compound amotosalen has been used to reduce the pathological effects of *L. major* inoculation and the attenuation of virulence of *L. infantum* and *L. chagasi* promastigotes [21,22].

Olea europaea L. (Olive), the most well-known species of the genus *Olea*, is one of the most famous fruit crops all over the Middle East [23]. According to the previous studies, different parts of *O. europaea* have been used in folk medicine to remedy some illness [24]. Moreover, its pharmacological features such as antidiabetic, anticancer, anti-inflammatory, antihypertensive, antimicrobial, and antiparasitic effects have been attributed to this plant [25,26].

Pharmacological properties of *F. carica* Linn and *Olea europaea* L. (Olive) extracts has been scrutinized, with antimicrobial, antiparasitic, anti-inflammatory, and immunobalancing effects mainly due to the presence high level of flavonoids and polyphenols compounds that possess the strongest antioxidant potential effects [22,25,26].

In the present study, *Ficus carica* Linn (Fig) and *Olea europaea* (Olive) extracts with (Ag-NPs) exhibited remarkable antileishmanial property. This activity may be attributed to the presence of flavonoids and polyphenols compounds that acts as antileishmanial potency by enhancing scavenges free radicals that produced by *L. major* and by increasing the activity of antioxidant defense system.

Hence, we examined the efficacy of silver nanoparticles biosynthesized by using Fig (*Ficus carica* Linn) and Olive (*Olea europaea*) extracts against (*L. major*) induced inflammation in female Balb/c mice.

Materials and methods

Plant material and extract preparation

Dried fruits of *Ficus carica* were purchased from the local market in Riyadh. About 10 g of the dried fruit was crushed, incubated for 10 min in 100 ml distilled water at 60°C and filtered through Whatman no.1 filter paper (pore size 25 mm). The filtrate was further filtered through 0.6 mm sized filters. The resulting filtrate was immediately used for preparing (Ag-NPs) as previously described [19].

Fresh leaves of *Olea europaea* were collected from the Alhamedih farm owned by Almayouf Abdulhamid in Sakaka Aljouf, surface cleaned with running tap water to remove debris and other contaminated organic contents, followed by double distilled water and air dried at room temperature. About 10 g of crushed dried leaves were kept in a beaker containing 100 ml distilled water and incubated for 10 min at 60°C. The extract was cooled down and filtered with Whatman filter paper no.1 and the resulting extract was immediately used for preparing (Ag-NPs) as previously described [27].

Phenolic content

Total phenolic compound content of dried fruits for each *Ficus carica* and dried leaves of *Olea europaea* were assayed by the Folin-Ciocalteu method as described previously [28]. Briefly, 0.1 ml of the sample's extract was mixed with 2.5 ml of distilled water in a test tube, and then 0.1 ml of undiluted Folin-Ciocalteu reagent (Sigma-Aldrich, St. Louis, MO, U.S.A.) was added. The solution was mixed well and then allowed to stand for 6 min before adding 0.5 ml of

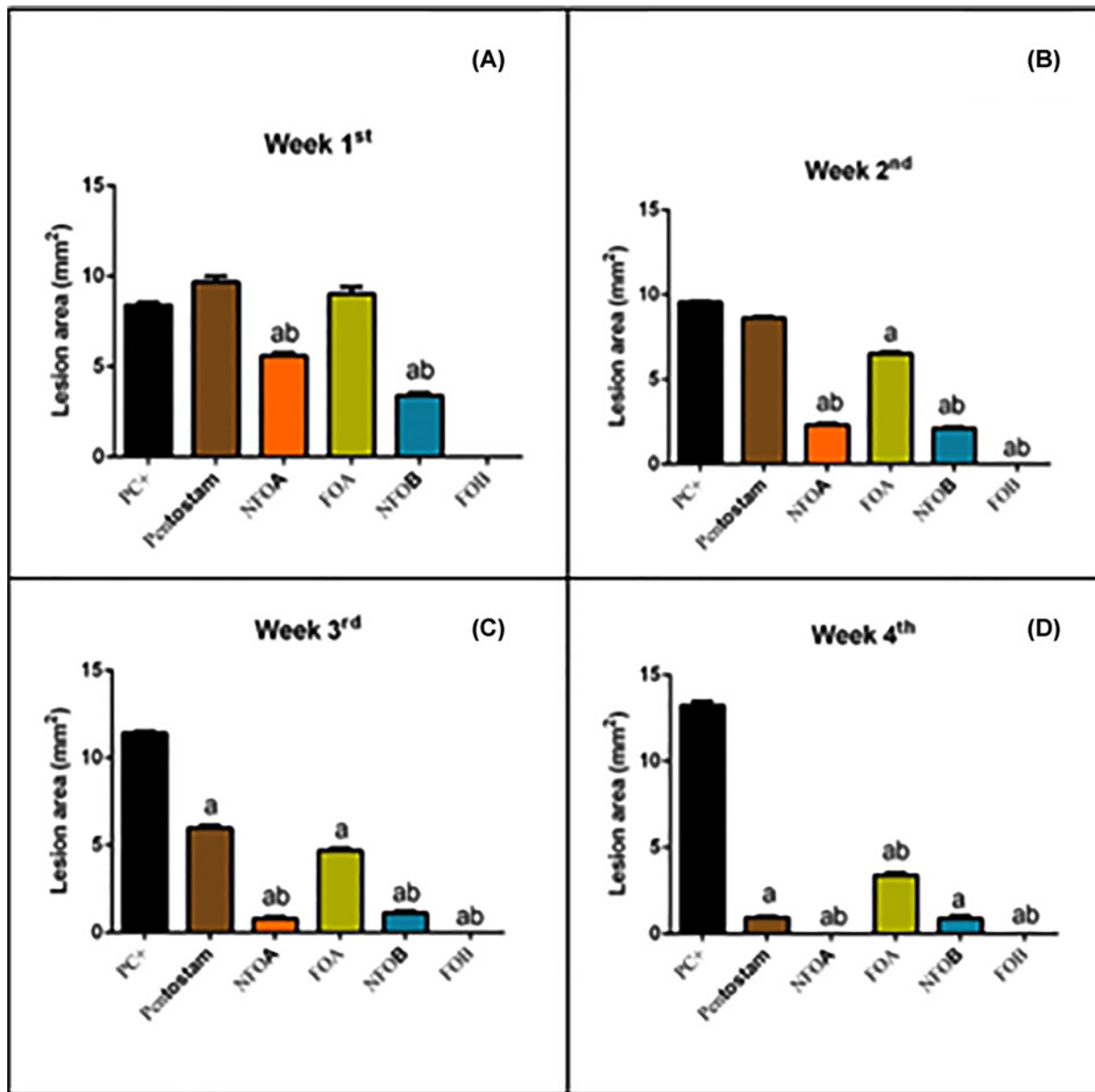


Figure 4. Determination CL lesion size

CL Lesion size in mouse skin one (A), two (B), three (C), and four (D) weeks after infection. Lesion sizes measured with a digital caliper as described in the 'Materials and Methods' section. Each point represents the mean \pm SD ($n=10$). Values are $c^a P < 0.05$, indicates statistically significant changes compared with negative control (NC) group; $b^b P < 0.05$ indicates statistically significant changes compared with PC group.

20% sodium carbonate solution. The color developed for 30 min at room (20°C) temperature and the absorbance was measured at 760 nm using a spectrophotometer (PD 303 UV spectrophotometer, Apel Co., Limited, Saitama, Japan). A blank sample was prepared using 0.1 ml of methanol instead of the extract. The measurement was compared to a calibration curve of gallic acid solution and expressed as milligram (mg) equivalent (eq.) of gallic acid per gram (g) of dry weight extract.

Flavonoids

The aluminum chloride colorimetric method was used to determine the total flavonoid content for each dried fruits of *Ficus carica* and dried leaves of *Olea europaea* as described previously [29]. Briefly, in a test tube, 50 μ l of the

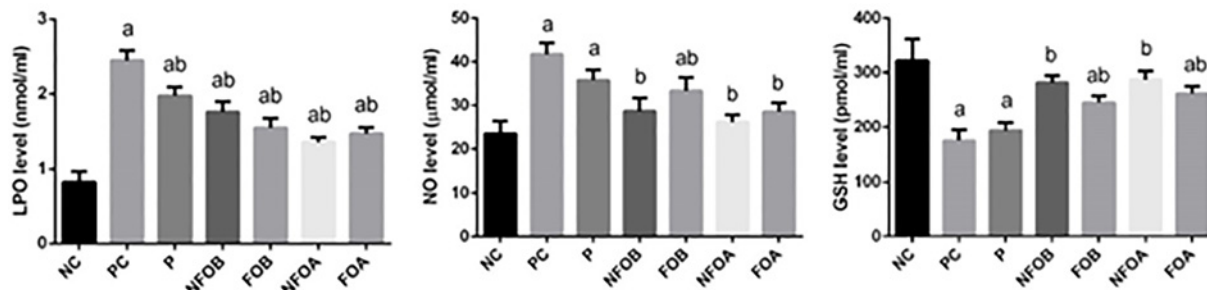


Figure 5. Determination of oxidative stress

Effect of Ag-NPs biosynthesized by (Fig and Olive) extracts pretreatment or posttreatment and Pentostam on oxidative stress markers LPO, NO, and GSH of control and experimental groups 4 weeks after infection. Values are mean \pm SD ($n=10$), ^a $P<0.05$, indicates statistically significant changes compared with negative control (NC) group; ^b $P<0.05$ indicates statistically significant changes compared with PC group. LPO, lipid peroxidation; NO, nitric oxide, and GSH, Glutathione.

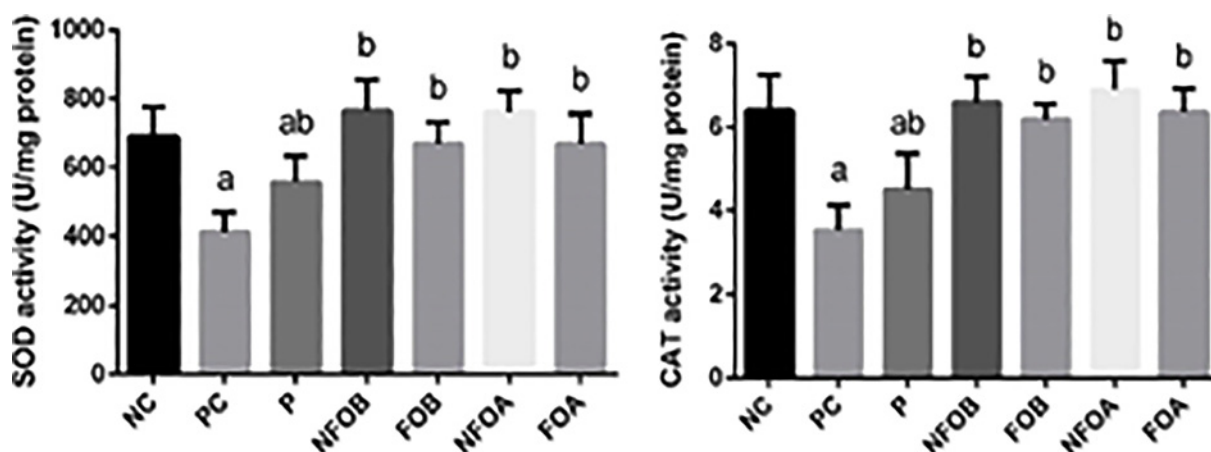


Figure 6. Determination enzymatic antioxidant status

Effect of Ag-NPs biosynthesized by (Fig and Olive) extracts pretreatment or post-treatment and Pentostam on dermal antioxidant enzyme activities (SOD, CAT) of control and experimental groups four weeks after infection. Values are mean \pm SD ($n=10$), ^a $P<0.05$ indicates statistically significant changes compared with NC group; ^b $P<0.05$ indicated statistically significant changes compared with PC group; SOD, superoxide dismutase; CAT, catalase.

extract was mixed with 4 ml of distilled water, 0.3 ml of 5% NaNO_2 solution, and 0.3 ml of 10% $\text{AlCl}_3 \cdot 6\text{H}_2\text{O}$. The mixture was allowed to stand for 6 min and then 2 ml of 1 mol/l NaOH solution was added; distilled water was subsequently added to bring the final volume to 10 ml. The mixture was allowed to stand for another 15 min and the absorbance was measured at 510 nm. The total flavonoid content was calculated from a calibration curve and the result is expressed as mg eq. rutin per g dry weight.

DPPH (2,2-diphenyl-1-picrylhydrazyl) radical scavenging activity

The power of the of dried fruits for each *Ficus carica* and dried leaves of *Olea europaea* to scavenge DPPH radicals was assayed as described previously [30]. A fresh solution of 0.08 mM DPPH radical in methanol was prepared. Next, 950 μl of DPPH solution was mixed with 50 μl extract and incubated for 5 min. Exactly 5 min later, the absorbance of the mixture was measured at 515 nm (PD 303 UV spectrophotometer, Apel Co., Limited). Antioxidant activity (AA) is expressed as percentage inhibition of DPPH radical using the equation below; $\text{AA} = 100 - [100 \times (\text{A sample}/\text{A control})]$, where A sample is the absorbance of the sample at time, $t = 5$ min and A control is the absorbance of the control.

ABTS [2,4,6-tri(2-pyridyl)-s-triazine] radical scavenging activity

The ABTS assay was used to determine the DPPH radical scavenging activity according to the method of Gouveia and Castilho (2011) [31]. The ABTS⁺ radical solution was prepared by reacting 50 ml of 2 mM ABTS solution with 200 μ l of 70 mM potassium persulfate solution. This mixture was stored in the dark for 16 h at room temperature and it was stable in this form for 2 days. For each analysis, the ABTS⁺ solution was diluted with pH 7.4 phosphate-buffered saline (PBS) solution to an initial absorbance of 0.700 ± 0.021 at 734 nm.

This solution was freshly prepared for each set of analysis. To determine the antiradical scavenging activity, an aliquot of 100 μ l methanolic solution was mixed with 1.8 ml of ABTS⁺ solution, and the decrease in absorbance at 734 nm (PD 303 UV spectrophotometer, Apel Co., Limited, Saitama, Japan) was recorded during 6 min. The results are expressed as μ mol Trolox equivalent per g of dried extract (μ mol eq. Trolox/g), based on the Trolox calibration curve.

Ferric reducing antioxidant power (FRAP)

Ferric reducing antioxidant power (FRAP) was performed as described previously [32]. The FRAP reagent included 300 mM acetate buffer, pH 3.6, 10 mM 2,4,6-Tris(2-pyridyl)-s-triazine (TPTZ) in 40 mM HCl, and 20 mM FeCl₃ in the ratio 10:1:1 (v/v/v). A volume of 3 ml of the FRAP reagent was mixed with 100 μ l of each dried fruits of *Ficus carica* and dried leaves of *Olea europaea* in a test tube and incubated with shaking at 37°C for 30 min in a water bath. Reduction of ferric-TPTZ to the ferrous complex formed an intense blue color, which was measured with a UV-visible spectrophotometer (PD 303 UV spectrophotometer, Apel Co., Limited) at 593 nm after 4 min. The results are expressed in terms of mol eq. Trolox per g of dried sample (μ mol eq. Trolox/g).

Synthesis of silver nanoparticles

Green silver nanoparticles were synthesized by bioreduction of Ag⁺ using fresh suspension of Fig and Olive extracts. About 5 ml of mixed extract was added drop by drop to an aqueous solution of AgNO₃ (50 ml, 0.1 mM/ml) and was stirred at 45–50°C for 30 min. Then, ultrasonication was applied to the mixed solution for 3 h. The colorless silver nitrate solution was changed to a deep brown solution, indicating the formation of (Ag-NPs). The residual AgNO₃ was removed by dialysis against deionized water at 4°C. The formed (Ag-NPs) were analyzed by Zeta sizer (ZEN 3600, Malvern, U.K.) and characterized using transmission electron microscopy (TEM) (JEM-1011, JEOL, Akishima, Japan). Furthermore, the green (Ag-NPs) synthesis was confirmed by using a UV-Vis spectrophotometer in the range of 200–1000 nm wavelength. The absorption spectra were recorded with Perkin-Elmer Lambda 40 B double beam spectrophotometer using 1 cm matched quartz cells. The stability of (Ag-NPs) was examined by observing the color of the solution after 20, 40, 50, and 60 days of storage at 4°C.

Leishmania major and culture

L. major promastigotes (MHOM/SA/84/JISH) of a Saudi substrain were maintained in RPMI1640 medium (GIBCO, New York, NY, U.S.A.) containing fetal bovine serum (FBS) (Sera Laboratories International, Horsted Keynes, U.K.), 100 U/ml penicillin + 100 mg/ml streptomycin (BioWhittaker, Verviers, Belgium), and 1% L-glutamine in 25 ml culture flasks. Each flask was incubated in an incubator at 25°C. Cultures were passaged after 4 days of incubation. Morphology and motility of promastigotes were observed by using an inverted microscope.

Experimental protocol

Balb/c female mice ($n=70$; eight weeks old) for the *in vivo* experiment were obtained from the animal house at the Female Center for Scientific and Medical colleges, Riyadh, KSA and the animal work has taken place in the Zoology Department, College of Science, King Saud University, Riyadh, KSA. Mice were challenged with *L. major* by subcutaneous injection of 0.1 ml of RPMI1640 media containing 10^7 promastigotes [33]. The animals were housed in wire-bottomed cages under standard conditions of illumination with a 12-h light-dark cycle and at a temperature of $25 \pm 1^\circ\text{C}$ for one week until the beginning of treatment. Animals were provided with tap water and a balanced diet ad libitum.

The animals were randomly divided into seven groups with 10 mice in each group, Group 1: (NC) Normal non-infected negative control group. Group 2: (PC) Infected untreated positive control group: Mice were subcutaneously inoculated with 1×10^7 promastigotes in a shaved area above the tail [33].

Group 3: (P) Infected mice treated with sodium stibogluconate (Pentostam) (Pen; 120 mg/kg intramuscularly) for 4 weeks starting with the first appearance of an ulcerative lesion [34], Group 4: (NFOB) Mice pretreated with oral (Fig and Olive) nanosilver (0.2 mg/mouse) 2 weeks before infection [35], Group 5: (FOB) Mice pretreated with oral

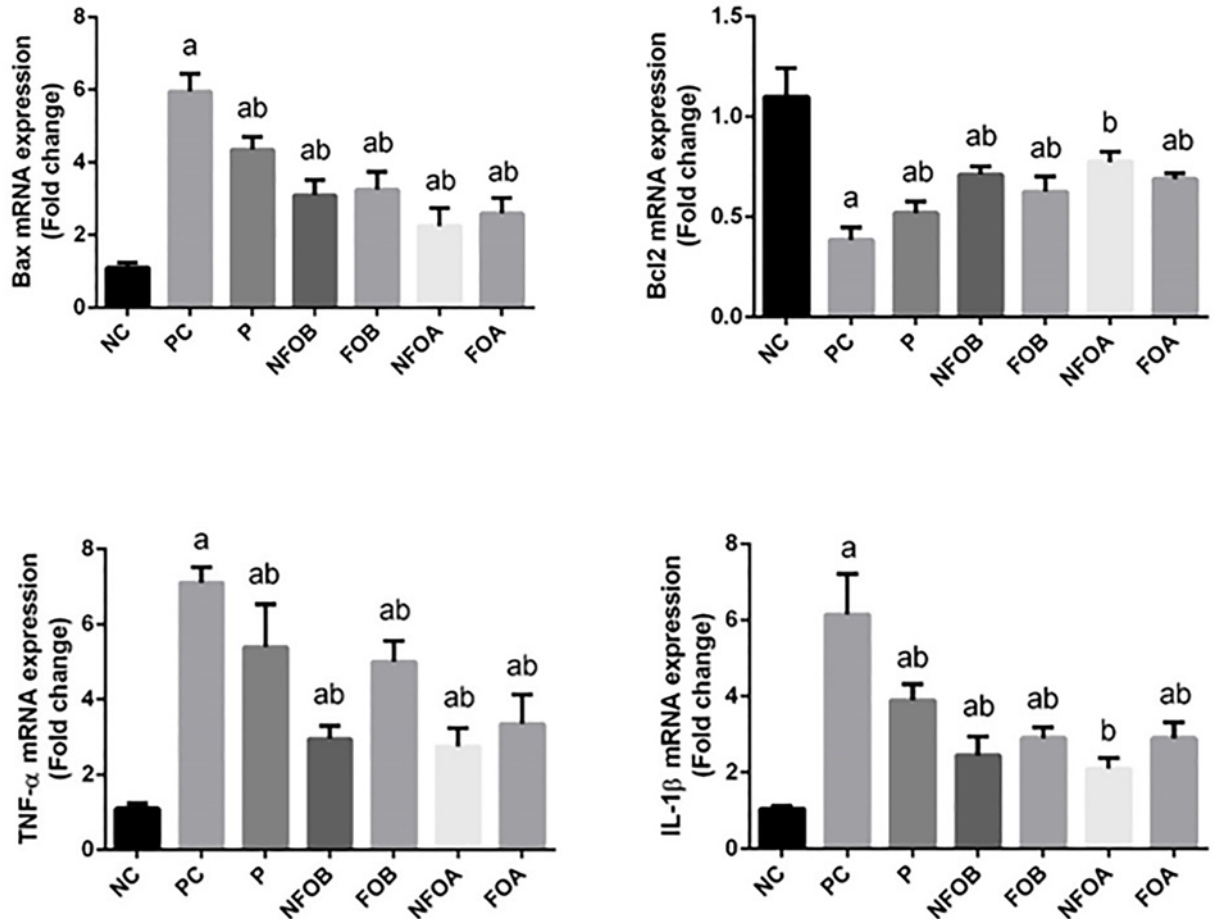


Figure 7. Gene expression profile by real-time PCR in skin

Effect of Ag-NPs biosynthesized by (Fig and Olive) extracts pretreatment or post-treatment and Pentostam on dermal pro-apoptotic and anti-apoptotic (*BAX* and *BCL-2*) and pro-inflammatory cytokines (*TNF-α* and *IL-1β*) in control and experimental groups. Values are mean \pm SD ($n=10$), ^a $P<0.05$ indicates statistically significant changes compared with NC group; ^b $P<0.05$ indicated statistically significant changes compared with PC group. BAX, BCL-2-associated X protein; BCL-2, B-cell lymphoma 2.

(Fig and Olive) (0.2 mg/mouse) 2 weeks before infection, Group 6: (NFOA) Infected mice treated with oral (Fig and Olive) nanosilver (0.2 mg/mouse) for 4 weeks starting with the first appearance of an ulcerative lesion, Group 7: (FOA) Infected mice treated with oral (Fig and Olive) (0.2 mg/mouse) for 4 weeks starting with the first appearance of an ulcerative lesion. Mortality was checked daily and parasitemia was assessed every other day by observing the appearance of lesions (2–6 weeks post-infection). Each week, the lesion size was measured before and after treatment with Vernier calipers in two diameters (a, b). The lesion size was calculated using the following formula [36]:

$$\text{Lesion Size (LS)} : \frac{a + b}{2}$$

Four weeks post-infection, mice were anaesthetized by CO₂, asphyxiation then sacrificed by guillotine and skin at the side of lesion was excised promptly. Skin samples for biochemical and molecular analysis were frozen at -80°C until processed.

Oxidative stress

Homogenates of the skin were prepared in 50 mM Tris-HCl and 300 mM sucrose to measure lipid peroxidation (LPO) in terms of the amount of malondialdehyde (MDA) formed using the thiobarbituric acid (TBA) method [37]. Whereas Green et al. [38] and Ellman methods [39] were applied to determine the levels of nitrite/nitrate (nitric oxide; NO).

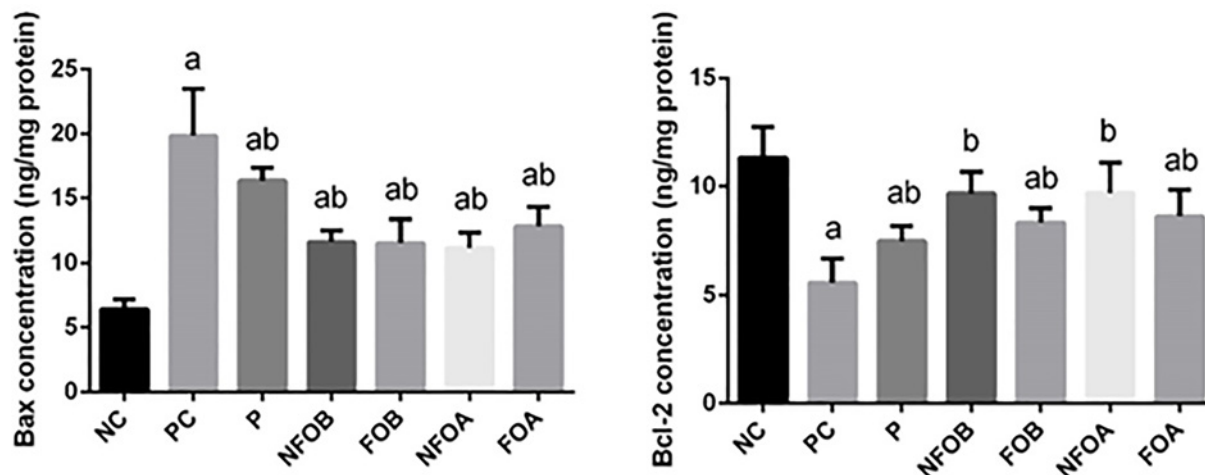


Figure 8. Determination of apoptotic markers in skin tissue

Effect of Ag-NPs biosynthesized by Fig and Olive extracts pretreatment or post-treatment and Pentostam on dermal pro-apoptotic and anti-apoptotic proteins (Bax and Bcl-2) in control and experimental groups. Values are mean \pm SD ($n=10$), ^a $P<0.05$ indicates statistically significant changes compared with NC group; ^b $P<0.05$ indicated statistically significant changes compared with PC group; BAX, BCL-2-associated X protein, BCL-2, B-cell lymphoma 2.

Enzymatic antioxidant status

The skin homogenates were also used to determine superoxide dismutase (SOD) [40], catalase (CAT) [41], and glutathione (GSH) according to the method of Ellman [39].

Real-time PCR

Total RNA was extracted from the skin tissue samples using a RNeasy plus Minikit (Qiagen, Valencia, CA, U.S.A.). RNA was reverse transcribed using the RevertAid H minus Reverse Transcriptase (Fermentas, Thermo Fisher Scientific Inc., Waltham, MA, U.S.A.). Real time PCR reactions were performed using Applied Biosystems 7500 Instrument. The relative gene expression was determined with power SYBR Green (Life Technologies, Carlsbad, CA, U.S.A.) and by the comparative threshold cycle method of Pfaffl [42]. The PCR primers for *BAX*, *BCL-2*, *TNF- α* , and *IL-1 β* genes were synthesized by Jena Bioscience GmbH (Jena, Germany). Primers were designed using the Primer-Blast program from NCBI.

mRNA levels for each sample were normalized to β -actin. The primer sets used the following:

Bax (S): 50- GTT TCA TCC AGG ATC GAG CAG -30.
Bax (AS): 50- CAT CTT CTT CCA GAT GGT GA -30.
Bcl-2 (S): 50- CCT GTG GAT GAC TGA GTA CC -30.
Bcl-2 (AS): 50- GAG ACA GCC AGG AGA AAT CA -30.
TNF- α (S): 50- AGAACTCAGCGAGGACACCAA -30.
TNF- α (AS): 50- GCTTGGTGGTTTGCTACGAC -30.
IL-1 β (S): 50- GACTTCACCATGGAACCCGT -30.
IL-1 β (AS): 50- GGAGACTGCCCATCTCTCGAC -30.

Determination of apoptotic markers in skin tissue

Skin sample homogenates were prepared in lysis buffer and analyzed using a Colorimetric Caspase-3 Assay Kit (Sigma-Aldrich Co., Saint Louis, MO, U.S.A.), according to the manufacturer's instructions. Whereas, BCL-2 and BAX protein levels were determined in skin homogenates by using ELISA kits (R&D Systems Inc., Minneapolis, MN, U.S.A.), according to the manufacturer's instructions. Levels were expressed as ng/mg tissue protein.

Histological examination

The tissues were collected and immediately fixed with 10% buffered formalin and embedded in paraffin. Sections (4–5 μ m) were prepared and then stained with hematoxylin and eosin dye for photomicroscopic observations.

Table 1 Determination of total quantity of the phenolic and flavonoids content existing in Fig (*Ficus carica*)

Parameters	Mean \pm SD
Total phenols (mg eq. Gallic acid/g sample)	8.576 \pm 0.665
Total flavonoids (mg eq. Rutin/g sample) DPPH (%)	0.723 \pm 0.042
DPPH (%)	39.798 \pm 1.99
ABTS (.mol eq. Trolox/g sample)	3.568 \pm 0.025
FRAB (.mol eq. Trolox/g sample)	0.102 \pm 0.0004

Experimental determinations of total phenolic and flavonoids contents and antioxidant capacity assays (ABTS, DPPH, and FRAB) for *Ficus carica*

Table 2 Determination of total quantity of the phenolic and flavonoids content existing in Olive (*Olea europaea*)

Parameters	Mean \pm SD
Total phenols (mg eq. Gallic acid/g sample)	13.457 \pm 1.245
Total flavonoids (mg eq. Rutin/g sample) DPPH (%)	0.998 \pm 0.0689
DPPH (%)	37.235 \pm 1.98
ABTS (.mol eq. Trolox/g sample)	6.756 \pm 0.0562
FRAB (.mol eq. Trolox/g sample)	0.278 \pm 0.0015

Experimental determinations of total phenolic and flavonoids contents and antioxidant capacity assays (ABTS, DPPH, and FRAB) for *Olea europaea*

Statistical analysis

Results are represented as means \pm standard deviation of the means (SD). Data were analyzed by one-way analysis of variance (ANOVA). For the comparison of significance between groups, Duncan's test was used as post hoc test according to the Statistical Package for the Social Sciences (SPSS version 20.0 IBM, Armonk, NY, U.S.A.).

Results

The total quantity of the phenolic and flavonoids content existing in the investigated extracts for each *Ficus carica* and *Olea europaea* was shown in Tables 1 and 2, which was found to be 8.576 \pm 0.665 mg eq. gallic acid/g, 0.723 \pm 0.042 mg eq. rutin/g, 13.457 \pm 1.245 and 0.998 \pm 0.0689, respectively. Moreover, the results exposed that the both *Ficus carica* and *Olea europaea* have powerful free radical scavenging power. For the DPPH, ABTS, and FRAB assays, the values obtained were of 39.798 \pm 1.99, 3.568 \pm 0.025 0.102 \pm 0.0004, 37.235 \pm 1.98, 6.756 \pm 0.0562, and 0.278 \pm 0.0015 mol eq. Trolox/g, respectively.

A UV-visible spectrophotometer was used in order to confirm the presence of NFO. As shown in Figure 1A, the appearance of a band around 300 nm indicates the formation of NFO. In order to determine the size of the biosynthesized NFO particle, Zeta analysis was performed to determine the average particle diameter in nanometer (d.nm). NFO size distribution is shown in Figure 1B. The size of NFO particles ranged from 51 to 226 d.nm with an average size of 103.1 d.nm. Furthermore, TEM (Figure 2) demonstrated that most NFO were obviously spherical or polygonal in morphology, with a size ranging from 50 to 100 nm. Interestingly, after 50 days of storage at 4°C, the color of the NFO aqueous solution did not change indicating their stability. However, the color changed into colorless after 60 days.

Next, we examined whether concurrent treatment or pretreatment of mice with (NFO) could protect from *L. major* infection. Clinically, lesions in (PC) mice showed redness and swelling at the site of *L. major* inoculation at the fourth week post infection (Figure 3A,B).

In the infected control mice, the mean lesion size increased gradually by the fourth week following infection. It was observed that the lesion size started to decrease gradually after NFOA treatment was initiated and at the third week of treatment lesions had completely disappeared (Figure 4). CL infection significantly ($P < 0.05$) enhanced lipid peroxidation LPO and nitric oxide NO production whereas, the dermal glutathione content was depleted significantly compared with the control mice. NFOA treatment significantly reversed the increase in LPO and NO, and the GSH (glutathione) content was increased significantly indicating the antioxidant property of NFOA (Figure 5).

Chronic wounds often exhibit oxidative stress that slows down the wound-healing process, suppresses collagen deposition and epithelialization and enzymatic antioxidants that play crucial roles in accelerating wound-healing [43]. We found that *L. major* infection of mice inhibited significantly ($P < 0.05$) the antioxidant enzyme activities of superoxide dismutase (SOD) and catalase (CAT) (Figure 6). These biochemical findings were confirmed by the

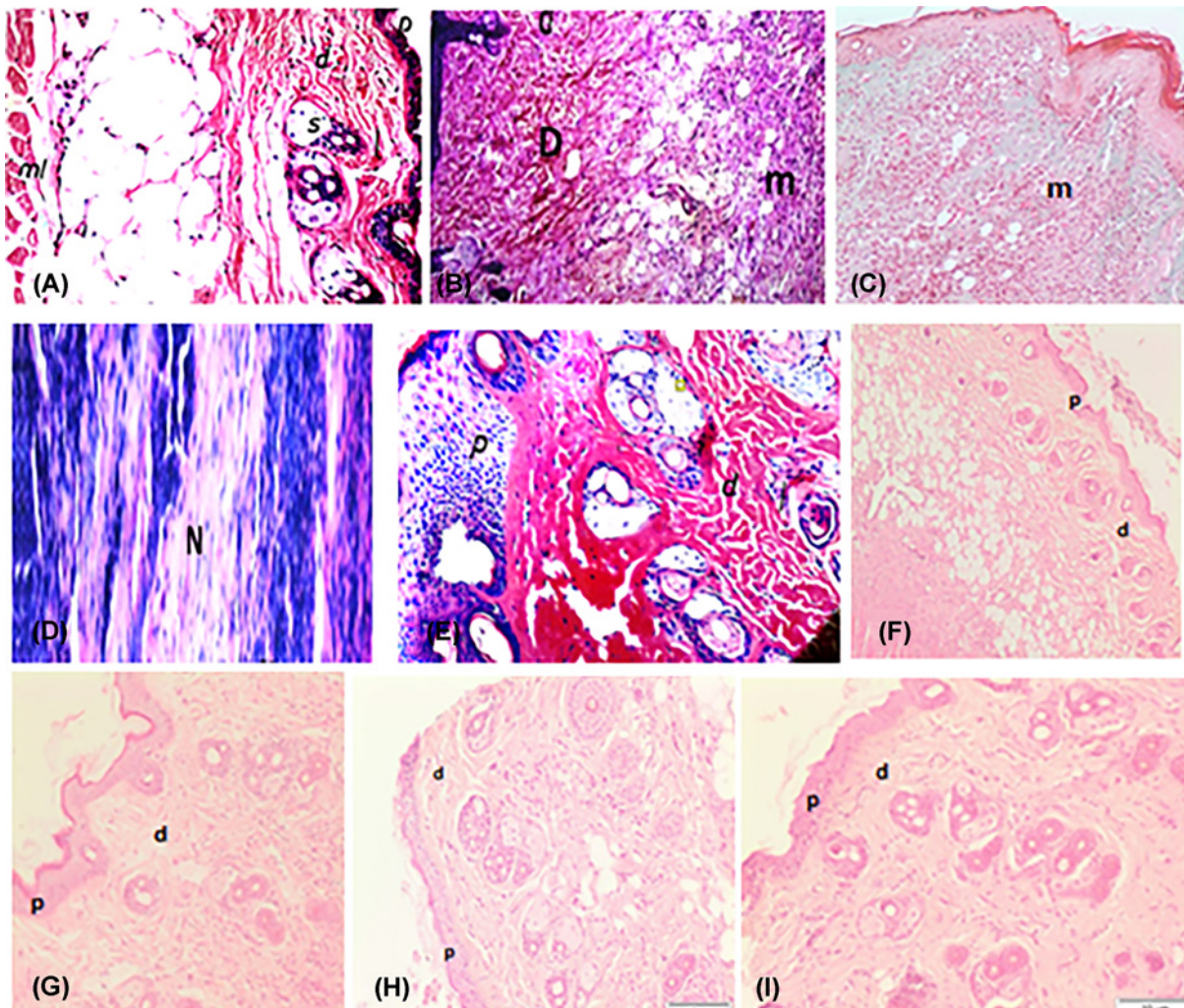


Figure 9. Examination of the histological changes in the skin of mice

Hematoxylin and eosin-stained skin sections. (A) Control animals showed no abnormalities, no histopathological alteration and normal histological structure of the epidermis, dermis, subcutaneous, and musculature tissue. (B and C) Skin section of the PC group at 4 weeks post-infection showing highly inflammatory cells infiltration in diffuse manner in subcutaneous tissue (m). (D and E) Pentostam treated mice at 4-week post-treatment showing acanthosis in the epidermis (P), while the underlying deep dermis and subcutaneous musculature showed inflammatory cells infiltration. No histopathological alteration in both epidermal and dermal layers. (E) Skin of mice showing suppurative liquefactive necrosis in deep subcutaneous tissue (N). (F) Mice treated orally with (NFOA) at the third week post-treatment, showing an intact epidermis (p) and dermis (d) with remarkable reduction in the inflammatory response. (G) Mice received orally treatment (NFOB) two weeks before infection, showing normal histological structure of epidermis (P) and dermis (D) and few inflammatory cells infiltration in dermal and subcutaneous tissue. (H) Mice treated only with (FOA) showed normal histological structure of epidermis and dermis and few inflammatory cells infiltration in dermal and subcutaneous tissue. (I) Mice received (FOB) daily 2 weeks before infection, showing normal histological structure of epidermis and dermis and few inflammatory cells infiltration in dermal and subcutaneous tissue.

molecular analyses. NFOA treatment promoted the activity of the antioxidant enzymes and these enzymes showed higher activities than those in *L. major* infection mice. Furthermore, the results revealed that post treatment with NFOA led to better outcomes and Pentostam has no antioxidant activity.

To investigate whether the observed anti-*leishmaniasis* effects of NFO were related to their anti-apoptotic activity, the protein levels of *BCL-2* and *BAX* in dermal tissue were measured. The expression levels of the anti-apoptotic protein *BCL-2* were significantly reduced ($P < 0.05$), while those of the pro-apoptotic protein *BAX* were increased

in *L. major* infected mice (Figure 7). However, mice treated with NFO concurrently or prior to *L. major* infection showed a significant increase in *BCL-2* and a significant decrease in *BAX*.

The present study also showed a significant up-regulation in the expression of *IL-1 β* and *TNF- α* mRNA following infection with *L. major* compared with the control group. In contrast, treatment with NFO (pre. and post.) caused a significant decrease in the expression levels of *TNF- α* and *IL-1 β* mRNAs (Figure 7).

To investigate whether the observed anti-*leishmaniasis* effects of NFO were related to the anti-apoptotic activity of NFO, the protein levels of Bcl-2 and Bax in dermal tissue were measured. The current findings revealed that the anti-apoptotic protein Bcl-2 was significantly reduced ($P < 0.05$), while the pro-apoptotic protein Bax was increased in *L. major* infection mice (Figure 8). However, mice treated with NFO concurrently or prior to *L. major* infection showed significant increase of Bcl-2 and decreased significantly the Bax level.

Examination of the histological changes in the skin of mice from all the groups supported the results observed from the previous experiments (Figure 9). Four weeks after infection, the skin of infected mice showed a moderately dense, localized dermal infiltrate composed of mixed acute and chronic nonspecific inflammatory cellular infiltrates. Congested dilated blood vessels were observed, and numerous *Leishmania* promastigotes were seen either inside or outside the macrophages. Moreover, suppurative liquefactive necrosis was observed in deep subcutaneous tissue. In Pentostam-treated mice, the skin showed normal histological structure of subcutaneous musculature tissue and infiltration of few inflammatory cells in the subcutaneous tissue. However, apparent ameliorations were noticed. In the NFOA group, the tissue sections showed an intact epidermis with a moderately dense infiltrate, milder grade of infection in terms of both the inflammatory response and the number of visible amastigotes. Furthermore, the intensity of infection was also less than that of the infected untreated controls. Surprisingly, no sign of pathological changes was found in mice NFOB pretreated and those treated with NFOA.

Discussion

Green synthesis nanoparticles are a great interest, since their large-scale application in the biomedical sector (nanomedicine). This is due to synthesized by green technologies in the size range from 1 to 100 nanometers exhibit antioxidant, anti-inflammatory, and immunomodulatory activities. A distinctive feature of the nanoparticle's synthesis with use plants called (phytosynthesis) due to a higher rate of nanoparticle formation and contains a wide range of biomolecules such as, (poly) phenolic and flavonoids compounds [44,45].

In the present study, the plants species of Figs and Olives were as a source for the synthesis of Ag-NPs. The formation of NFO was confirmed by the change in color and the stability in the solution. TEM analysis determined that the range of particle size was about 100 nm and that they were spherical in shape. The flavonoids, polyphenols, and other constituents present in the extracts of Figs and Olives act as the surface-active stabilizing molecules for the synthesis of (Ag-NPs) with antioxidative and anti-inflammatory activities [46].

In the present study, we demonstrate that *Ficus carica* Linn (Fig) and *Olea europaea* (Olive) extracts with (Ag-NPs) improved skin lesions and promote their healing and parasite resolution in Balb/c mice infected with *L. major*. This activity may be attributed to the presence of phenolic and flavonoids compounds that possesses antileishmanial potency by enhancing nonspecific immunity by macrophages activation and inducing NO, interferon-gamma and tumor necrosis factor-gamma, so those chemicals and cytokines produce fundamental host defense system and kill the invading parasite [47,48].

NFOA treatment caused a significant reduction in the average lesion size and complete healing after 21 days compared with standard drug Pentostam that needs more than 28 days for healing. This is in accordance with previous reports [49–53].

Reactive oxygen species (ROS) formed during multiple normal processes in tissues and cells are involved in the pathogenesis of various parasitic infections including *Leishmania* spp., *Toxoplasma gondii*, *Giardia lamblia*, and *Entamoeba histolytica* [54–57]. *Leishmania* *L. major* induce inflammation by mast cell stimulation and by secreting proinflammatory mediators. ROS that are produced during an inflammatory response lead to oxidative injury to noninfected cells. During oxidative damage, released free radicals play an important role in collagen damage [58–61].

The overproduction of NO levels in response to parasitic infection may be considered as one of the factors inducing oxidative stress and inflecting tissue injury [62]. Finally, NO production correlates positively with tissue fibrosis through inducing fibrogenic cytokines and increasing collagen synthesis [63–65].

In our study, CL infection impaired the antioxidant system, GSH is the main endogenous antioxidants, was depleted and associated with lipid peroxidation, a marker of cellular oxidative stress. In the present study, an elevation in MDA, the product of LPO in infected and Pentostam groups, was observed. LPO has been traditionally thought to be the major effect of free radicals. It leads to impairment in the physicochemical properties of the membrane including

its fluidity and integrity and to the induction of apoptosis [66]. Treatment with NFOA increased the GSH content [64], and subsequently reduced the formation of intracellular ROS in response to different pro-oxidant stimuli [67]. The present data suggest that NFOB is capable of protecting cells by stabilizing the membrane permeability through inhibiting LPO and preventing GSH depletion.

The activities of antioxidant enzymes SOD and CAT in the skin tissue of mice infected with CL also decreased; CAT detoxifies hydrogen to water while SOD catalyzes the reduction of superoxide anions to hydrogen peroxide [68].

To explore the mechanism by which NFO attenuate CL-induced apoptosis, the levels of BAX and BCL-2 protein were measured in skin homogenates. ROS have been shown to increase the permeability of the mitochondrial membrane and to result in mitochondrial failure [69–72]. The permeability of the mitochondrial membrane is dependent upon the mitochondrial permeability transition pore that mediates the release of cytochrome *c* from the mitochondria to the cytosol [73]. Once released, cytochrome *c* can bind to apoptotic protease-activating factor-1 (Apaf-1) in the cytoplasm forming a complex that can activate caspase-9 with subsequent induction of death [66,74,75]. The mitochondria-mediated intrinsic apoptotic pathway is controlled by BCL-2 family proteins. The BCL-2 protein family is classified into two subgroups according to structural homology: the anti-apoptotic proteins such as BCL-2, BCL-XL, and the pro-apoptotic proteins such as BAX and Bak. The balance between the pro- and anti-apoptotic proteins of the BCL-2 family is important to determine cell survival or death. BCL-2 has also been found to function as a counteracting force to reduce the damage mediated by LPO triggered by cytotoxic stimuli such as ROS [76,77]. BCL-2 was also found to prevent the release of cytochrome *c*. In contrast, BAX regulates apoptosis, not only by dimerizing with anti-apoptotic BCL-2 proteins, but also by regulating cytochrome *c* release and subsequent caspase-3 activation [78–80]. The present study also showed that treatment of mice with NFO reversed the CL-induced alternations in BCL-2 and BAX levels, and substantially restored the ratio of BCL-2/BAX. In the current report, NFO inhibited all toxic events induced by CL. It is known that extracts with silver nanoparticles scavenge oxygen and nitrogen reactive species generated in mitochondria, stabilize the mitochondrial membrane and enhance anti-apoptotic signaling.

Inflammation is characterized by the release of proinflammatory cytokines such as TNF- α , IL-1 β , and IL-6, as well as inflammatory mediators, including nitric oxide (NO) and prostaglandin E2 (PGE2), which are synthesized by inducible nitric oxide synthase (iNOS) and cyclooxygenase (COX). These inflammatory mediators and cytokines are involved in the causation of many human diseases including rheumatoid arthritis, asthma, atherosclerosis, infections, and endotoxin-induced multiple organ injury [81–83]. Anti-inflammatory agents reduce the inflammatory response by suppressing the production of inflammatory cytokines and mediators [84,85].

During infection, the inflammation is a response by macrophages to effect healing and restoration. The kinetics of the responses of proinflammatory, anti-inflammatory cytokines, and inflammatory master regulator nuclear factor- κ B (NF- κ B) elicited by pathogen-associated molecular patterns, such as lipopolysaccharide (LPS), and virulence factors are microbial inducers of inflammation which is may be critical determinants of the inflammatory response by macrophages [86].

The production of these cytokines typically proceeds via host cell signaling cascades following the engagement of innate pathogen-associated molecular pattern (PAMP) receptors including the Toll-like receptors (TLRs) expressed primarily by cells of the innate immune compartment and by pathogen-specific ligands, such as LPS [87].

The exposure of macrophages to *Leishmania* leads to the generation of ROS, which contribute to the regulation of the inflammatory response controlled by the cellular antioxidant defense system [88,89].

NF- κ B has a seminal role in immunity, because it induced the expression of pro-inflammatory genes encoding *iNOS*, *COX-2*, *TNF- α* , *IL-1 β* , and *IL-6* [85,90]. It is activated by phosphorylation, ubiquitination, and subsequent proteolytic degradation of the I κ B protein by activated I κ B kinase (IKK) [91]. The liberated NF- κ B translocates to the nucleus and binds as a transcription factor to κ B motifs in the promoters of target genes, leading to their transcription. Aberrant NF- κ B activity is associated with various inflammatory diseases, and most anti-inflammatory drugs suppress inflammatory cytokine expression by inhibiting the NF- κ B pathway [92,93]. Thus, an NF- κ B inhibitor has clinical potential in inflammatory diseases.

The lipopolysaccharides receptor, LPS, interacts with the small GTP-binding protein Rac1, and then associates with p47phox and p67phox (two subunits needed for NADPH oxidase p91phox function) at the cell membrane, leading to ROS production [94].

Our findings demonstrate that the natural product nanoparticles inhibited signaling cascade of proinflammatory gene expression in LPS-stimulated macrophages by suppressing NF- κ B activation, probably as a result of scavenging intracellular ROS. This inhibitory effect has important implications for the development of anti-inflammatory drugs and strategies to limit pathological inflammation [95–97].

The present study showed a significant up-regulation in the *TNF- α* , *IL-1 β* , and *BAX* genes expression levels caused by *leishmania* infection, while *BCL-2* gene was up-regulated in mice treated with NFOA compared with the control

group. In contrast with our data, it has been reported that nanoparticles cause a significant decrease in the expression of *TNF- α* , *IL-1 β* , and *BAX* genes. This is in agreement with previous reports [98,99].

Conclusions

These findings indicated that Ag-NPs biosynthesized from Fig and Olive extracts could be considered as a safe chemotherapeutic agent, for fast treatment of *Leishmaniasis* and complete healing after 21 days compared with standard drug Pentostam (needs more than 28 days for healing). It could be a possible new anti-leishmanial drug against *Leishmania major*.

Competing Interests

The authors declare that there are no competing interests associated with the manuscript.

Funding

The author declares that there are no sources of funding to be acknowledged.

Author Contribution

M.A. and M.E. conceived and designed the experiments. M.A. performed the experiments. M.A., M.E., and E.A. analyzed the data. M.A. and E.A. contributed reagents/materials/analysis tools. M.A. and M.E. wrote the paper.

Acknowledgements

The authors would like to thank Mr. Almayouf Abdulhamid for providing the Olive leaves.

Abbreviations

BAX, BCL-2-associated X protein; BCL-2, B-cell lymphoma 2; COX, cyclooxygenase; iNOS, inducible nitric oxide synthase; NO, nitric oxide; PAMP, pathogen-associated molecular pattern; PGE2, prostaglandin E2; ROS, reactive oxygen species; SOD, superoxide dismutase; TLR, Toll-like receptor.

References

- Ilango, K. (2010) A taxonomic reassessment of the *Phlebotomus argentipes* species complex (Diptera: Psychodidae: Phlebotominae). *J. Med. Entomol.* **47**, 1–5, <https://doi.org/10.1093/jmedent/47.1.1>
- Zilberstein, D. (2008) Physiological and biochemical aspects of *Leishmania* development. *Leishmania after the Genome* **1**, 107–122
- Tolouei, S., Hejazi, S.H., Ghaedi, K. and Hashemini, S.J. (2014) Identification of *Leishmania* isolates from healing and nonhealing cutaneous leishmaniasis patients using internal transcribed spacer region PCR. *Jundishapur J. Microbiol.* **7**, 12–38, <https://doi.org/10.5812/jjm.9529>
- Bennis, I., Thys, S., Filali, H., De Brouwere, V., Sahibi, H. and Boelaert, M. (2017) Psychosocial impact of scars due to cutaneous leishmaniasis on high school students in Errachidia province, Morocco. *Infectious Dis. Poverty* **6**, 46, <https://doi.org/10.1186/s40249-017-0267-5>
- de Menezes, J.P., Guedes, C.E., Petersen, A.L., Fraga, D.B. and Veras, P.S. (2015) Advances in development of new treatment for leishmaniasis. *BioMed Res. Int.* **2015**, 1–12, <https://doi.org/10.1155/2015/815023>
- Suleiman, A.K. (2014) Attitudes and beliefs of consumers of herbal medicines in Riyadh, Saudi Arabia. *J. Community Med. Health Educ.* **4**, 269
- Dias, D.A., Urban, S. and Roessner, U. (2012) A historical overview of natural products in drug discovery. *Metabolites* **2**, 303–336, <https://doi.org/10.3390/metabo2020303>
- Harvey, A.L., Edrada-Ebel, R. and Quinn, R.J. (2015) The re-emergence of natural products for drug discovery in the genomics era. *Nat. Rev. Drug Discovery* **14**, 111–129, <https://doi.org/10.1038/nrd4510>
- Zhang, Y., Cheng, X., Zhang, Y., Xue, X. and Fu, Y. (2013) Biosynthesis of silver nanoparticles at room temperature using aqueous aloe leaf extract and antibacterial properties. *Colloids Surf. A* **423**, 63–68, <https://doi.org/10.1016/j.colsurfa.2013.01.059>
- Kulkarni, N. and Muddapur, U. (2014) Biosynthesis of metal nanoparticles: a review. *J. Nanotechnol.* **2014**, 1–9, <https://doi.org/10.1155/2014/510246>
- Mohamed, H.E., Afridi, S., Khalil, A.T., Zia, D., Iqbal, J., Ullah, I. et al. (2019) Biosynthesis of silver nanoparticles from *Hyphaene thebaica* fruits and their in vitro pharmacognostic potential. *Mater. Res. Express* **6**, 1050c9, <https://doi.org/10.1088/2053-1591/ab4217>
- Shanmuganathan, R., Karuppusamy, I., Saravanan, M., Muthukumar, H., Ponnuchamy, K., Ramkumar, V.S. et al. (2019) Synthesis of Silver nanoparticles and their biomedical applications-A comprehensive review. *Curr. Pharm. Des.* **25**, 2650–2660, <https://doi.org/10.2174/1381612825666190708185506>
- Shekhawat, M.S., Manokari, M., Kannan, N., Revathi, J. and Latha, R. (2013) Synthesis of silver nanoparticles using *Cardiospermum halicacabum* L. leaf extract and their characterization. *J. Phytopharmacol.* **2**, 15–20
- Kang, S.N., Goo, Y.M., Yang, M.R., Ibrahim, R.I., Cho, J.H., Kim, I.S. et al. (2013) Antioxidant and antimicrobial activities of ethanol extract from the stem and leaf of *Impatiens balsamina* L. (Balsaminaceae) at different harvest times. *Molecules* **18**, 6356–6365, <https://doi.org/10.3390/molecules18066356>

- 15 Parwanto, M.E., Senjaya, H. and Edy, H.J. (2013) Formulasi Salep Antibakteri Ekstrak Etanol Daun Tembelekan (*lantana camara* L). *Pharmacol* **2**, 104–108
- 16 Kyriazis, I.D., Koutsoni, O.S., Aligiannis, N., Karampetsou, K., Skaltsounis, A.L. and Dotsika, E. (2016) The leishmanicidal activity of oleuropein is selectively regulated through inflammation-and oxidative stress-related genes. *Parasites Vectors* **9**, 1–6, <https://doi.org/10.1186/s13071-016-1701-4>
- 17 Rao, C.V., Verma, A.R., Vijayakumar, M. and Rastogi, S. (2008) Gastroprotective effect of standardized extract of *Ficus glomerata* fruit on experimental gastric ulcers in rats. *J. Ethnopharmacol.* **115**, 323–326, <https://doi.org/10.1016/j.jep.2007.09.019>
- 18 Chawla, A., Kaur, R. and Sharma, A.K. (2012) *Ficus carica* Linn.: A review on its pharmacognostic, phytochemical and pharmacological aspects. *Int. J. Pharmaceut. Phytopharmacol. Res.* **1**, 215–232
- 19 Jacob, S.J., Prasad, V.S., Sivasankar, S. and Muralidharan, P. (2017) Biosynthesis of silver nanoparticles using dried fruit extract of *Ficus carica*—Screening for its anticancer activity and toxicity in animal models. *Food Chem. Toxicol.* **109**, 951–956, <https://doi.org/10.1016/j.fct.2017.03.066>
- 20 Anasdas, J.R., Kannaiyan, P., Raghavachary, R., Gopinath, S.C. and Chen, Y. (2018) Palladium nanoparticle-decorated reduced graphene oxide sheets synthesized using *Ficus carica* fruit extract: A catalyst for Suzuki cross-coupling reactions. *PLoS ONE* **13**, e0193281, <https://doi.org/10.1371/journal.pone.0193281>
- 21 Didwania, N., Shadab, M., Sabur, A. and Ali, N. (2017) Alternative to Chemotherapy—The Unmet Demand against Leishmaniasis. *Front. Immunol.* **8**, 1779, <https://doi.org/10.3389/fimmu.2017.01779>
- 22 Yeganeh, F. and Hoseini, M.H. (2017) Current Approaches to Develop a Live Vaccine against *Leishmania major*. *Novelty Biomed.* **5**, 133–137
- 23 Kaniewski, D., Van Campo, E., Boiy, T., Terral, J.F., Khadari, B. and Besnard, G. (2012) Primary domestication and early uses of the emblematic olive tree: palaeobotanical, historical and molecular evidence from the Middle East. *Biol. Rev.* **87**, 885–899, <https://doi.org/10.1111/j.1469-185X.2012.00229.x>
- 24 Hashmi, M.A., Khan, A., Hanif, M., Farooq, U. and Perveen, S. (2015) Traditional uses, phytochemistry, and pharmacology of *Olea europaea* (olive). *Evidence-Based Complement. Altern. Med.* **2015**, 1–29, <https://doi.org/10.1155/2015/541591>
- 25 Saedi Dezaki, E., Mahmoudvand, H., Shariffar, F., Fallahi, S., Monzote, L. and Ezatkhah, F. (2016) Chemical composition along with anti-leishmanial and cytotoxic activity of *Zataria multiflora*. *Pharm. Biol.* **54**, 752–758, <https://doi.org/10.3109/13880209.2015.1079223>
- 26 Kheirandish, F., Mahmoudvand, H., Khamesipour, A., Ebrahimzadeh, F., Behrahi, F., Rezaei, S. et al. (2017) The therapeutic effects of olive leaf extract on *Leishmania major* infection in BALB/c mice. *Marmara Pharmaceut. J.* **21**, 837–842, <https://doi.org/10.12991/mpj.2017.6>
- 27 Ahmed, S., Saifullah, A.M., Swami, B.L. and Ikram, S. (2016) Green synthesis of silver nanoparticles using *Azadirachta indica* aqueous leaf extract. *J. Radiation Res. Applied Sci.* **9**, 1–7, <https://doi.org/10.1016/j.jrras.2015.06.006>
- 28 Wu, C.H., Murthy, H.N., Hahn, E.J. and Paek, K.Y. (2007) Improved production of caffeic acid derivatives in suspension cultures of *Echinacea purpurea* by medium replenishment strategy. *Arch. Pharm. Res.* **30**, 945–949, <https://doi.org/10.1007/BF02993961>
- 29 Baba, S.A. and Malik, S.A. (2015) Determination of total phenolic and flavonoid content, antimicrobial and antioxidant activity of a root extract of *Arisaema jacquemontii* Blume. *J. Taibah University Sci.* **9**, 449–454, <https://doi.org/10.1016/j.jtusci.2014.11.001>
- 30 Akillioglu, H.G. and Karakaya, S. (2010) Changes in total phenols, total flavonoids, and antioxidant activities of common beans and pinto beans after soaking, cooking, and in vitro digestion process. *Food Sci. Biotechnol.* **19**, 633–639, <https://doi.org/10.1007/s10068-010-0089-8>
- 31 Gouveia, S. and Castilho, P.C. (2011) Antioxidant potential of *Artemisia argentea* L'Hér alcoholic extract and its relation with the phenolic composition. *Food Res. Int.* **44**, 1620–1631, <https://doi.org/10.1016/j.foodres.2011.04.040>
- 32 Benzie, I.F. and Strain, J.J. (1996) The ferric reducing ability of plasma (FRAP) as a measure of “antioxidant power”: the FRAP assay. *Anal. Biochem.* **239**, 70–76, <https://doi.org/10.1006/abio.1996.0292>
- 33 Belkaid, Y., Kamhawi, S., Modi, G., Valenzuela, J., Noben-Trauth, N., Rowton, E. et al. (1998) Development of a natural model of cutaneous leishmaniasis: powerful effects of vector saliva and saliva preexposure on the long-term outcome of *Leishmania major* infection in the mouse ear dermis. *J. Exp. Med.* **188**, 1941–1953, <https://doi.org/10.1084/jem.188.10.1941>
- 34 Kuhlencord, A., Maniera, T., Eibl, H. and Unger, C. (1992) Hexadecylphosphocholine: oral treatment of visceral leishmaniasis in mice. *Antimicrob. Agents Chemother.* **36**, 1630–1634, <https://doi.org/10.1128/AAC.36.8.1630>
- 35 Maes, L., Berghe, D.V., Germonprez, N., Quirijnen, L., Cos, P., De Kimpe, N. et al. (2004) In vitro and in vivo activities of a triterpenoid saponin extract (PX-6518) from the plant *Maesa balansae* against visceral *Leishmania* species. *Antimicrob. Agents Chemother.* **48**, 130–136, <https://doi.org/10.1128/AAC.48.1.130-136.2004>
- 36 Ashraf, J.M., Ansari, M.A., Khan, H.M., Alzohairy, M.A. and Choi, I. (2016) Green synthesis of silver nanoparticles and characterization of their inhibitory effects on AGEs formation using biophysical techniques. *Sci. Rep.* **6**, 20414, <https://doi.org/10.1038/srep20414>
- 37 Ohkawa, H., Ohishi, N. and Yagi, K. (1979) Assay for lipid peroxides in animal tissues by thiobarbituric acid reaction. *Anal. Biochem.* **95**, 351–358, [https://doi.org/10.1016/0003-2697\(79\)90738-3](https://doi.org/10.1016/0003-2697(79)90738-3)
- 38 Green, L.C., Wagner, D.A., Glogowski, J., Skipper, P.L., Wishnok, J.S. and Tannenbaum, S.R. (1982) Analysis of nitrate, nitrite, and [15N] nitrate in biological fluids. *Anal. Biochem.* **126**, 131–138, [https://doi.org/10.1016/0003-2697\(82\)90118-X](https://doi.org/10.1016/0003-2697(82)90118-X)
- 39 Ellman, G.L. (1959) Tissue sulfhydryl groups. *Arch. Biochem. Biophys.* **82**, 70–77, [https://doi.org/10.1016/0003-9861\(59\)90090-6](https://doi.org/10.1016/0003-9861(59)90090-6)
- 40 Nishikimi, M., Rao, N.A. and Yagi, K. (1972) The occurrence of superoxide anion in the reaction of reduced phenazine methosulfate and molecular oxygen. *Biochem. Biophys. Res. Commun.* **46**, 849–854, [https://doi.org/10.1016/S0006-291X\(72\)80218-3](https://doi.org/10.1016/S0006-291X(72)80218-3)
- 41 Aebi, H. (1984) [13] Catalase in vitro. *Methods in enzymology*, vol. 105, pp. 121–126, Academic Press, [https://doi.org/10.1016/S0076-6879\(84\)05016-3](https://doi.org/10.1016/S0076-6879(84)05016-3)
- 42 Pfaffl, M.W. (2001) A new mathematical model for relative quantification in real-time RT–PCR. *Nucleic Acids Res.* **29**, e45, <https://doi.org/10.1093/nar/29.9.e45>

- 43 Honnegowda, T.M., Kumar, P., Udupa, P., Rao, P., Bhandary, S., Mahato, K.K. et al. (2014) Effect of limited access dressing on hydroxyproline and enzymatic antioxidant status in nonhealing chronic ulcers. *Indian J. Plastic Surg.: Off. Publication Assoc. Plastic Surgeons of India* **47**, 216, <https://doi.org/10.4103/0970-0358.138952>
- 44 Farag, R.S., El-Baroty, G.S. and Basuny, A.M. (2003) Safety evaluation of olive phenolic compounds as natural antioxidants. *Int. J. Food Sci. Nutr.* **54**, 159–174, <https://doi.org/10.1080/0963748031000136306>
- 45 Solomon, A., Golubowicz, S., Yablownicz, Z., Grossman, S., Bergman, M., Gottlieb, H.E. et al. (2006) Antioxidant activities and anthocyanin content of fresh fruits of common fig (*Ficus carica* L.). *J. Agric. Food Chem.* **54**, 7717–7723, <https://doi.org/10.1021/jf060497h>
- 46 Misganaw, D., Engidawork, E. and Nedi, T. (2019) Evaluation of the anti-malarial activity of crude extract and solvent fractions of the leaves of *Olea europaea* (Oleaceae) in mice. *BMC Complement. Alternative Med.* **19**, 171, <https://doi.org/10.1186/s12906-019-2567-8>
- 47 Kolodziej, H., Kayser, O., Kiderlen, A.F., Ito, H., Hatano, T., Yoshida, T. et al. (2001) Antileishmanial activity of hydrolyzable tannins and their modulatory effects on nitric oxide and tumour necrosis factor- α release in macrophages in vitro. *Planta Med.* **67**, 825–832, <https://doi.org/10.1055/s-2001-18850>
- 48 Iqbal, K., Iqbal, J., Staerk, D. and Kongstad, K.T. (2017) Characterization of antileishmanial compounds from *Lawsonia inermis* L. leaves using semi-high resolution antileishmanial profiling combined with HPLC-HRMS-SPE-NMR. *Front. Pharmacol.* **8**, 337, <https://doi.org/10.3389/fphar.2017.00337>
- 49 Zeyrek, F.Y., Korkmaz, M. and Özbel, Y. (2007) Serodiagnosis of anthroponotic cutaneous leishmaniasis (ACL) caused by *Leishmania tropica* in Sanliurfa Province, Turkey, where ACL is highly endemic. *Clin. Vaccine Immunol.* **14**, 1409–1415, <https://doi.org/10.1128/0133-07>
- 50 Awaad, A.S., Al-Zaylaee, H.M., Alqasoumi, S.I., Zain, M.E., Aloyan, E.M., Alafeefy, A.M. et al. (2014) Anti-leishmanial Activities of Extracts and Isolated Compounds from *Drechslera rostrata* and *Eurotium tonopholium*. *Phytother. Res.* **28**, 774–780, <https://doi.org/10.1002/ptr.5096>
- 51 Alkathiri, B., El-Khadragy, M.F., Metwally, D.M., Al-Olayan, E.M., Bakhrebah, M.A. and Abdel Moneim, A.E. (2017) Pomegranate (*Punica granatum*) juice shows antioxidant activity against cutaneous leishmaniasis-induced oxidative stress in female BALB/c mice. *Int. J. Environ. Res. Public Health* **14**, 1592, <https://doi.org/10.3390/ijerph14121592>
- 52 El-khadragy, M., Alolayan, E.M., Metwally, D.M., El-Din, M.F., Alobud, S.S., Alsultan, N.I. et al. (2018) Clinical efficacy associated with enhanced antioxidant enzyme activities of silver nanoparticles biosynthesized using *Moringa oleifera* leaf extract, against cutaneous leishmaniasis in a murine model of *Leishmania major*. *Int. J. Environ. Res. Public Health* **15**, 1037, <https://doi.org/10.3390/ijerph15051037>
- 53 Singh, B., Buckner, F.S. and Pollastri, M.P. (2019) Discovery of Drugs for Leishmaniases: A Progress Report. *Neglected Tropical Diseases: Drug Discovery Development* 60–139, <https://doi.org/10.1002/9783527808656.ch6>
- 54 Yazar, S., Kilic, E., Saraymen, R. and Sahin, I. (2003) Serum malondialdehyde levels in *Toxoplasma* seropositive patients. *Ann. Saudi Med.* **23**, 413–415, <https://doi.org/10.5144/0256-4947.2003.413>
- 55 Demirci, M., Delibas, N., Altuntas, I., Oktem, F. and Yönden, Z. (2003) Serum iron, zinc and copper levels and lipid peroxidation in children with chronic giardiasis. *J. Health Popul. Nutr.* 72–75
- 56 Sim, S., Yong, T.S., Park, S.J., Im, K.I., Kong, Y., Ryu, J.S. et al. (2005) NADPH oxidase-derived reactive oxygen species-mediated activation of ERK1/2 is required for apoptosis of human neutrophils induced by *Entamoeba histolytica*. *J. Immunol.* **174**, 4279–4288, <https://doi.org/10.4049/jimmunol.174.7.4279>
- 57 Quaresma, J.A. (2019) Organization of the skin Immune system and compartmentalized immune responses in infectious diseases. *Clin. Microbiol. Rev.* **32**, e00034–18, <https://doi.org/10.1128/CMR.00034-18>
- 58 Sakhthianandeswaren, A., Elso, C.M., Simpson, K., Curtis, J.M., Kumar, B., Speed, T.P. et al. (2005) The wound repair response controls outcome to cutaneous leishmaniasis. *Proc. Natl. Acad. Sci.* **102**, 15551–15556, <https://doi.org/10.1073/pnas.0505630102>
- 59 Kocyigit, A., Gurel, M. and Ulukanligil, M. (2003) Erythrocyte antioxidative enzyme activities and lipid peroxidation levels in patients with cutaneous leishmaniasis. *Parasite* **10**, 277–281, <https://doi.org/10.1051/parasite/2003103277>
- 60 Rodríguez, N.E. and Wilson, M.E. (2014) Eosinophils and mast cells in leishmaniasis. *Immunol. Res.* **59**, 129–141, <https://doi.org/10.1007/s12026-014-8536-x>
- 61 Šmidová, B. The role of nitric oxide in mice infected with *Trichobilharzia regenti*, the neuropathogenic schistosome. *Charles University, Faculty of Science, Department of Parasitology* Diploma thesis
- 62 Jafari, M., Shirbazou, S. and Norozi, M. (2014) Induction of oxidative stress in skin and lung of infected BALB/C mice with Iranian strain of *Leishmania major* (MRH0/IR/75/ER). *Iranian J. Parasitol.* **9**, 60
- 63 Parola, M. and Robino, G. (2001) Oxidative stress-related molecules and liver fibrosis. *J. Hepatol.* **35**, 297–306, [https://doi.org/10.1016/S0168-8278\(01\)00142-8](https://doi.org/10.1016/S0168-8278(01)00142-8)
- 64 Asmaa, Q., Salwa, A.S., Al-Tag, M., Adam, A.S., Li, Y. and Osman, B.H. (2017) Parasitological and biochemical studies on cutaneous leishmaniasis in Shara'b District, Taiz, Yemen. *Ann. Clin. Microbiol. Antimicrobials* **16**, 47, <https://doi.org/10.1186/s12941-017-0224-y>
- 65 Jafari, M., Shirbazou, S., Sadraie, S.H., Kaka, G. and Norozi, M. (2015) The role of apoptosis in the cellular response of liver and spleen of BALB/c mice in cutaneous leishmaniasis. *Iranian J. Med. Sci.* **40**, 133
- 66 Pamplona, R. (2008) Membrane phospholipids, lipoxidative damage and molecular integrity: a causal role in aging and longevity. *Biochim. Biophys. Acta (BBA)-Bioenergetics* **1777**, 1249–1262, <https://doi.org/10.1016/j.bbabi.2008.07.003>
- 67 Ernst, E. (2000) Adverse effects of herbal drugs in dermatology. *Br. J. Dermatol.* **143**, 923–929, <https://doi.org/10.1046/j.1365-2133.2000.03822.x>
- 68 Allahverdiyev, A.M., Abamor, E.S., Bagirova, M., Ustundag, C.B., Kaya, C., Kaya, F. et al. (2011) Antileishmanial effect of silver nanoparticles and their enhanced antiparasitic activity under ultraviolet light. *Int. J. Nanomed.* **6**, 2705, <https://doi.org/10.2147/IJN.S23883>
- 69 Matés, J.M. and Sánchez-Jiménez, F.M. (2000) Role of reactive oxygen species in apoptosis: implications for cancer therapy. *Int. J. Biochem. Cell Biol.* **32**, 157–170, [https://doi.org/10.1016/S1357-2725\(99\)00088-6](https://doi.org/10.1016/S1357-2725(99)00088-6)
- 70 Getti, G. *Interaction between Leishmania parasites and mammalian macrophages*, University of Greenwich, Doctoral dissertation

- 71 Huang, S.H., Lin, C.M. and Chiang, B.H. (2008) Protective effects of *Angelica sinensis* extract on amyloid β -peptide-induced neurotoxicity. *Phytomedicine* **15**, 710–721, <https://doi.org/10.1016/j.phymed.2008.02.022>
- 72 Wajihullah, K.H. and Zakai, H.A. (2014) Epidemiology, pathology and treatment of cutaneous leishmaniasis in Taif region of Saudi Arabia. *Iranian J. Parasitol.* **9**, 365
- 73 Yang, W., Shi, L., Chen, L., Zhang, B., Ma, K., Liu, Y. et al. (2014) Protective effects of perindopril on d-galactose and aluminum trichloride induced neurotoxicity via the apoptosis of mitochondria-mediated intrinsic pathway in the hippocampus of mice. *Brain Res. Bull.* **109**, 46–53, <https://doi.org/10.1016/j.brainresbull.2014.09.010>
- 74 Ghribi, O., Herman, M.M. and Savory, J. (2002) The endoplasmic reticulum is the main site for caspase-3 activation following aluminum-induced neurotoxicity in rabbit hippocampus. *Neurosci. Lett.* **324**, 217–221, [https://doi.org/10.1016/S0304-3940\(02\)00147-7](https://doi.org/10.1016/S0304-3940(02)00147-7)
- 75 Al-Olayan, E.M., El-Khadragy, M.F. and Abdel Moneim, A.E. (2015) The protective properties of melatonin against aluminium-induced neuronal injury. *Int. J. Exp. Pathol.* **96**, 196–202, <https://doi.org/10.1111/iep.12122>
- 76 Akifusa, S., Kamio, N., Shimazaki, Y., Yamaguchi, N., Nishihara, T. and Yamashita, Y. (2009) Globular adiponectin-induced RAW 264 apoptosis is regulated by a reactive oxygen species-dependent pathway involving Bcl-2. *Free Radic. Biol. Med.* **46**, 1308–1316, <https://doi.org/10.1016/j.freeradbiomed.2009.02.014>
- 77 Pimple, B.P. and Badole, S.L. (2014) Polyphenols: A remedy for skin wrinkles. *Polyphenols in Human Health and Disease*, pp. 861–869, Academic Press
- 78 Gavrilescu, L.C. and Denkers, E.Y. (2003) Apoptosis and the balance of homeostatic and pathologic responses to protozoan infection. *Infect. Immun.* **71**, 6109–6115, <https://doi.org/10.1128/IAI.71.11.6109-6115.2003>
- 79 Cai, X., Zhang, H., Tong, D., Tan, Z., Han, D., Ji, F. et al. (2011) Corosolic acid triggers mitochondria and caspase-dependent apoptotic cell death in osteosarcoma MG-63 cells. *Phytother. Res.* **25**, 1354–1361, <https://doi.org/10.1002/ptr.3422>
- 80 Bacellar, I.O., Tsubone, T.M., Pavani, C. and Baptista, M.S. (2015) Photodynamic efficiency: from molecular photochemistry to cell death. *Int. J. Mol. Sci.* **16**, 20523–20559, <https://doi.org/10.3390/ijms160920523>
- 81 Ritchlin, C.T., Haas-Smith, S.A., Li, P., Hicks, D.G. and Schwarz, E.M. (2003) Mechanisms of TNF- α - and RANKL-mediated osteoclastogenesis and bone resorption in psoriatic arthritis. *J. Clin. Invest.* **111**, 821–831, <https://doi.org/10.1172/JCI200316069>
- 82 Sommer, C. and Kress, M. (2004) Recent findings on how proinflammatory cytokines cause pain: peripheral mechanisms in inflammatory and neuropathic hyperalgesia. *Neurosci. Lett.* **361**, 184–187, <https://doi.org/10.1016/j.neulet.2003.12.007>
- 83 Carruthers, V.B. and Suzuki, Y. (2007) Effects of *Toxoplasma gondii* infection on the brain. *Schizophr. Bull.* **33**, 745–751, <https://doi.org/10.1093/schbul/sbm008>
- 84 Leach, M., Hamilton, L.C., Olbrich, A., Wray, G.M. and Thiemermann, C. (1998) Effects of inhibitors of the activity of cyclo-oxygenase-2 on the hypotension and multiple organ dysfunction caused by endotoxin: a comparison with dexamethasone. *Br. J. Pharmacol.* **124**, 586–592, <https://doi.org/10.1038/sj.bjp.0701869>
- 85 Makarov, S.S. (2000) NF- κ B as a therapeutic target in chronic inflammation: recent advances. *Mol. Med. Today* **6**, 441–448, [https://doi.org/10.1016/S1357-4310\(00\)01814-1](https://doi.org/10.1016/S1357-4310(00)01814-1)
- 86 Adamson, A., Boddington, C., Downton, P., Rowe, W., Bagnall, J., Lam, C. et al. (2016) Signal transduction controls heterogeneous NF- κ B dynamics and target gene expression through cytokine-specific refractory states. *Nat. Commun.* **7**, 1–4, <https://doi.org/10.1038/ncomms12057>
- 87 Arnold, L., Henry, A., Poron, F., Baba-Amer, Y., Van Rooijen, N., Plonquet, A. et al. (2007) Inflammatory monocytes recruited after skeletal muscle injury switch into antiinflammatory macrophages to support myogenesis. *J. Exp. Med.* **204**, 1057–1069, <https://doi.org/10.1084/jem.20070075>
- 88 Baer, M., Dillner, A., Schwartz, R.C., Sedon, C., Nedospasov, S. and Johnson, P.F. (1998) Tumor necrosis factor alpha transcription in macrophages is attenuated by an autocrine factor that preferentially induces NF- κ B p50. *Mol. Cell. Biol.* **18**, 5678–5689, <https://doi.org/10.1128/MCB.18.10.5678>
- 89 Berg, D.J., Kühn, R., Rajewsky, K., Müller, W., Menon, S., Davidson, N. et al. (1995) Interleukin-10 is a central regulator of the response to LPS in murine models of endotoxic shock and the Shwartzman reaction but not endotoxin tolerance. *J. Clin. Invest.* **96**, 2339–2347, <https://doi.org/10.1172/JCI118290>
- 90 De Vera, M.E., Shapiro, R.A., Nussler, A.K., Mudgett, J.S., Simmons, R.L., Morris, S.M. et al. (1996) Transcriptional regulation of human inducible nitric oxide synthase (NOS2) gene by cytokines: initial analysis of the human NOS2 promoter. *Proc. Natl. Acad. Sci.* **93**, 1054–1059, <https://doi.org/10.1073/pnas.93.3.1054>
- 91 De Martin, R., Vanhove, B., Cheng, Q., Hofer, E., Csizmadia, V., Winkler, H. et al. (1993) Cytokine-inducible expression in endothelial cells of an I kappa B alpha-like gene is regulated by NF kappa B. *EMBO J.* **12**, 2773–2779, <https://doi.org/10.1002/j.1460-2075.1993.tb05938.x>
- 92 Castrillo, A., De las Heras, B., Hortelano, S., Rodriguez, B., Villar, A. and Boscá, L. (2001) Inhibition of the nuclear factor κ B (NF- κ B) pathway by tetracyclic kaurene diterpenes in macrophages specific effects on NF- κ B-inducing kinase activity and on the coordinate activation of erk and p38 MAPK. *J. Biol. Chem.* **276**, 15854–15860, <https://doi.org/10.1074/jbc.M100010200>
- 93 Keifer, J.A., Guttridge, D.C., Ashburner, B.P. and Baldwin, A.S. (2001) Inhibition of NF- κ B activity by thalidomide through suppression of I κ B kinase activity. *J. Biol. Chem.* **276**, 22382–22387, <https://doi.org/10.1074/jbc.M100938200>
- 94 Sanlioglu, S., Williams, C.M., Samavati, L., Butler, N.S., Wang, G., McCray, P.B. et al. (2001) Lipopolysaccharide induces Rac1-dependent reactive oxygen species formation and coordinates tumor necrosis factor- α secretion through IKK regulation of NF- κ B. *J. Biol. Chem.* **276**, 30188–30198, <https://doi.org/10.1074/jbc.M102061200>
- 95 Bai, S.K., Lee, S.J., Na, H.J., Ha, K.S., Han, J.A., Lee, H. et al. (2005) β -Carotene inhibits inflammatory gene expression in lipopolysaccharide-stimulated macrophages by suppressing redox-based NF- κ B activation. *Exp. Mol. Med.* **37**, 323–334, <https://doi.org/10.1038/emm.2005.42>

- 96 Kim, J.Y., Park, S.J., Yun, K.J., Cho, Y.W., Park, H.J. and Lee, K.T. (2008) Isoliquiritigenin isolated from the roots of *Glycyrrhiza uralensis* inhibits LPS-induced iNOS and COX-2 expression via the attenuation of NF- κ B in RAW 264.7 macrophages. *Eur. J. Pharmacol.* **584**, 175–184, <https://doi.org/10.1016/j.ejphar.2008.01.032>
- 97 Park, H.J., Jeong, S.K., Kim, S.R., Bae, S.K., Kim, W.S., Jin, S.D. et al. (2009) Resveratrol inhibits *Porphyromonas gingivalis* lipopolysaccharide-induced endothelial adhesion molecule expression by suppressing NF- κ B activation. *Arch. Pharm. Res.* **32**, 583–591, <https://doi.org/10.1007/s12272-009-1415-7>
- 98 Zhou, X., Smith, J.A., Oi, F.M., Koehler, P.G., Bennett, G.W. and Scharf, M.E. (2007) Correlation of cellulase gene expression and cellulolytic activity throughout the gut of the termite *Reticulitermes flavipes*. *Gene* **395**, 29–39, <https://doi.org/10.1016/j.gene.2007.01.004>
- 99 Heimesaat, M.M., Karadas, G., Alutis, M., Fischer, A., Kühl, A.A., Breithaupt, A. et al. (2015) Survey of small intestinal and systemic immune responses following murine *Arcobacter butzleri* infection. *Gut Pathogens* **7**, 1–1, <https://doi.org/10.1186/s13099-015-0075-z>